Water Environment Federation
the water quality people

Removal of total dissolved solids from wastewater using a revolving algal biofilm reactor

Juan Peng ,[1,2] Kuldip Kumar ,[3]* Martin Gross ,[4]* Thomas Kunetz ,[3]* Zhiyou Wen [2,4,]*

[1]Guangdong Provincial Key Laboratory of Marine Resources and Coastal Engineering, School of Marine Sciences, Sun Yat-Sen University, Guangzhou, China

[2]Department of Food Science and Human Nutrition, Iowa State University, Ames, Iowa

[3]Metropolitan Water Reclamation District of Greater Chicago, Chicago, Illinois

[4]Gross-Wen Technologies Inc., Ames, Iowa

Received 14 July 2019; Revised 2 November 2019; Accepted 6 November 2019

Metropolitan Water Reclamation District of Greater Chicago, Grant/Award Number: 14-062-AP

Correspondence to: Zhiyou Wen, Department of Food Science and Human Nutrition, Iowa State University, Ames, IA. Email: wenz@iastate.edu

*WEF Member/fellow

Published online 3 December 2019 in Wiley Online Library (wileyonlinelibrary.com)

DOI: 10.1002/wer.1273

Abstract

Total dissolved solids (TDS) comprising inorganic salts and organic matters are pollutants of concern to aquatic systems and water for human use. This work aimed to investigate the use of revolving algal biofilm (RAB) reactors as a sustainable and environmental friendly method to remove TDS from industrial effluents and municipal wastewaters. The wastewaters contained chloride, sodium, potassium, calcium, magnesium, and sulfate as the major components. The RAB reactors fed with synthetic industrial effluent with high TDS level demonstrated the best algal growth, with the highest TDS removal efficiency (27%) and removal rate (2,783 mg/L-day and 19,530 mg/m^2-day). A suspended algal culture system only removed 3% TDS from the same wastewater. The TDS removal by the RAB reactors was considered due to several mechanisms such as absorption by the algae cells, adsorption by extracellular polymeric substance of the biofilm, and/or precipitation. Collectively, this research shows that the RAB reactors can serve as an efficient system in wastewater remediation for TDS removal. © 2019 Water Environment Federation

Practitioner points

- Total dissolved solids (TDS) in wastewater are pollutants of concern.
- The RAB reactors can remove TDS from various types of wastewater.
- The RAB reactors removed TDS by adsorbing ions elements such as Cl, Na, K, Ca, Mg, and S.
- The algal biomass absorbs ions through extracellular polymeric substance.

Key words

chloride; extracellular polymeric substance; revolving algal biofilm; total dissolved solids

Introduction

Total dissolved solids (TDS) are generally comprised of inorganic salts (such as chloride, calcium, magnesium, potassium, sodium, bicarbonates, and sulfates) and organic matters dissolved in water (Zhang, Zhang, Huang, & Gao, 2017). Natural waterbodies commonly contain a certain level of TDS, but human activities such as agriculture, water use, urbanization, de-icing salt applications, and mining can significantly exacerbate the TDS level in surface and ground waters (Canedo-Arguelles et al., 2013; Steele & Aitkenhead-Peterson, 2011). This excess TDS can be toxic to many aquatic life such as fish, insects, amphibians, and macro-invertebrates. For example, TDS level above 250 mg/L can affect salmonid fertilization (Brix, Gerdesa, Curryc, Kaspera, & Grosella, 2010); increasing TDS from 270 to 1,170 mg/L can eliminate almost all coontail (*Ceratophyllus demersum*) and cattails (*Typha* sp.) from the ecosystem (Weber-Scannell & Duffy, 2007). Chapman, Bailey, and Canaria (2000) reported the chronic toxic effects such as reduced growth or survival in the chironomid larvae when TDS is over 1,100 mg/L. TDS-related acute toxicity was also reported to the water flea *Ceriodaphnia dubia* and the fish *Pimephales promelas, and* as a matter of

fact, these two aquatic animals have been used as test organism for TDS-related toxicity (Kennedy, Cherry, & Currie, 2003).

In the United States, TDS discharge limit for wastewater has been increasingly implemented at State levels (Pinto et al., 2016). For example, the State of Ohio has an average TDS limit of 1,500 mg/L to protect aquatic life, and 500 mg/L (average) and 750 mg/L (maximum) for public water supply as a protection of human health. In Iowa, chloride is used as the indicator to regulate TDS level with a standard of 250 mg/L of chloride in drinking water (Iowa DNR, 2009). In addition to municipal water, industrial effluents with high TDS level are also facing challenges of meeting TDS discharge limit before discharging into local municipal water resource recovery facilities under the US EPA pretreatment rules (USEPA, 2011).

Various methods such as physical adsorption, reverse osmosis (RO), distillation, precipitation, membrane filtration, and bacteria-based bioremediation have been developed to reduce/remove TDS from water streams (Pinto et al., 2016). Most of those methods, however, are not cost-effective and/or environmental friendly. For example, physical adsorption can only remove ions from water at certain capacity before the adsorbent reaches saturation and needs to be regenerated. RO is not economical and requires high energy with the issue of filter fouling and brine disposal. Distillation produces low conductivity water but the process is very energy-intensive due to a large amount of latent heat required. Biological absorption avoids the addition of chemicals but the process is often limited by the low rate of absorption by microbial cells.

Compared to the existing methods, biological absorption by microalgae is a mild and environmental friendly method for TDS removal. Algal cells absorb TDS species as nutrients and minerals to support their physiology and metabolisms while reducing TDS in water (Cho, Luong, Lee, Oh, & Lee, 2011; Khan, Shamshad, Waqas, Nawab, & Ming, 2017; Krishnamoorthy, Manickam, & Muthukaruppan, 2019; Lutzu & Dunford, 2019; Renuka, Sood, Ratha, Prasanna, & Ahluwalia, 2013; Sydney et al., 2011; Zhou, Li, et al., 2012). A consortium of filamentous algae was reported to reduce TDS of sewage water from 1,120 to 806 mg/L over 6 days (Renuka, Sood, Ratha, Prasanna, & Ahluwalia, 2013). An isolated alga *Leptolyngbya* sp. JPMTW1 reduced TDS from 490 to 427 mg/L with 7 days (Maity et al., 2014). Khan et al. (2017) reported 79% TDS removal from industrial wastewater within 12 days. In oil and gas production wastewater treatment, algae can remove up to 65% TDS over 30 days (Lutzu & Dunford, 2019). Krishnamoorthy et al. (2019) used blue-green algae to treat distiller wastewater with 64%–80% TDS removal over 7 days.

In addition to TDS removal, the biomass produced from the algal reactors can be used for various applications such as fertilizer, bio-based chemicals, and biofuel production. For example, algal biomass produced from open pond (Kumar, Prajapati, Malik, & Vijay, 2017) or biofilm reactor (Choudhary, Prajapati, Kumar, Malik, & Pant, 2017) has been used for energy recovery through anaerobic digestion.

Although microalgae have been identified as a promising candidate for TDS removal, developing a cost-effective algal culture system is still challenging. The conventional algae cultivation systems such as open ponds or enclosed photobioreactors typically result in very low cell densities (e.g., 0.05 wt% in open ponds and 0.1–0.5 wt% in photobioreactors). To harvest algal cells from these systems, the cell suspension is usually concentrated through sedimentation followed with centrifugation, which usually results in 20%–25% of total operation costs (Davis, Aden, & Pienkos, 2011). To overcome the high biomass harvest cost, an attachment-based algal culture system, revolving algal biofilm (RAB) reactor, has been developed (Gross, Henry, Michael, & Wen, 2013; Gross, Mascarenhas, & Wen, 2015; Gross & Wen, 2018; Gross, Zhao, Mascarenhas, & Wen, 2016). In the RAB system, algal cells grow in an attachment material ("belt"), which rotates through the liquid medium to absorb nutrients, then rotates out of the water to facilitate light exposure, and gas (CO_2 and O_2) exchanges. Algal biofilm biomass can be harvested in situ by scraping, which significantly reduces the biomass harvesting cost. In addition, the vertical configuration of the revolving belt allows for greater surface area exposure to sunlight in a much smaller footprint compared to an open raceway pond. The RAB system increases the algae retention time by retaining the biomass on the attachment surface without being flushed out of the reactor. The algal cells on the biofilm can directly utilize CO_2 from the gas phase, avoiding the barrier of CO_2 gas–liquid transfer in suspended cultures.

From a TDS removal perspective, RAB reactors can also be effective to removing ions and dissolved organic compounds from wastewater. Algal biofilm contains extracellular polymeric substances (EPS), a 3-D polymer network to facilitate algal cells to adhere on the belt and interact with each other (Xiao & Zheng, 2016). In particular, the negatively charged functional groups (such as carboxyl, hydroxyl, and phosphoric groups) in the EPS can adsorb various salts and organic matters (Delattre, Pierre, Laroche, & Michaud, 2016; Sheng, Yu, & Li, 2010). This physically based adsorption, together with the biological assimilation by the biofilm cells, enables the RAB system to remove a wide spectrum of dissolve solids from wastewater. The aim of this work is to evaluate the TDS removal performance of the RAB systems. Wastewaters containing different types and strength of TDS were evaluated. The algal biomass and EPS compositions were also determined to provide an insight into the TDS removal mechanisms by the type of reactor.

Materials and Methods

Wastewater streams

Wastewaters representing typical industrial effluents and municipal wastewater were used. These wastewaters include (a) synthetic industrial effluent with low TDS strength (industrial WW–low TDS), (b) synthetic industrial effluent with high TDS strength (industrial WW–high TDS), (c) municipal wastewater (raw wastewater after coarse solids being screened out but before entering the 1st sedimentation basin) from Ames Water Pollution Control Plant in Ames, Iowa USA (Ames WW), and (d) Ames WW supplemented with 1,000 mg/L of sodium chloride (Ames WW + NaCl). The compositions of those wastewaters and preparation methods are provided in Table 1. The industrial WW with high/low TDS was used to

Table 1. The component of different wastewater sources[a]

COMPONENTS (MG/L)	WASTEWATER (WW) SOURCES			
	INDUSTRIAL WW–LOW TDS[b]	INDUSTRIAL WW–HIGH TDS[c]	AMES WW	AMES WW + NACL[d]
Sodium	417	1,601	88	425
Potassium	64	252	13	13
Calcium	368	1,359	80	79
Magnesium	97	324	17	16
Chloride	1,250	4,500	175	781
Sulfur	138	540	33	37
Nitrogen	14	56	26	26
Phosphorus	9	36	12	13
Silicon	23	92	Not added	Not added
BBM trace metal solution[e]	10 ml/L	10 ml/L	Not added	Not added
TDS	3,430	12,100	840	2,065
pH	9.60	9.80	7.89	7.92

[a]Industrial WW does not contain organic matter in this study. Ames WW organic content was within the range of 300–500 mg COD/L with ~0.4 BOD_5/COD ratio. The specific Ames WW sample used in this specific work was 375 mg COD/L with 0.42 BOD_5/COD ratio.

[b]The industrial WW–low TDS was prepared by dissolving 1,000 mg/L NaCl, 1,000 mg/L $CaCl_2$, 100 mg/L KNO_3, 500 mg/L $MgSO_4$, 100 mg/L $NaSiO_3$, 50 mg/L K_2HPO_4, and 10 ml/L BBM trace metal stock solution into water.

[c]The industrial WW–high TDS has the same component species with four times higher concentration than those in industrial WW–low TDS.

[d]Ames WW + NaCl was prepared by adding 1,000 mg/L sodium chloride into Ames WW.

[e]The composition of the BBM (Bold's Basal Medium) trace metal stock solution includes 97 mg/L $FeCl_3.6H_2O$, 41 mg/L $MnCl_2.4H_2O$, 5 mg/L $ZnCl_2$, 2 mg/L $CoCl_2.6H_2O$, and 4 mg/L $Na_2MoO_4.2H_2O$.

mimic the typical industrial effluents in Chicago area. The salt concentration in these effluents was prepared based on data commonly recorded by the Metropolitan Water Reclamation District (MWRD) of Greater Chicago. The Ames WW + NaCl was mimicking municipal wastewater with high salt content resulted from de-icing road salt use in winter. There will be certain bacterial growth (so as the bacteria-based TDS removal) due to the organic compounds it contained. Table 1 also shows that the pH of the wastewaters was within alkaline range from 7.9 to 9.8.

Microalgal seed cultures

The microalgal seed culture (0.5–1 g/L, dry basis) was maintained at a raceway pond (1,000 L working volume) at the Algal Production Facility at Iowa State University in Boone, IA, USA. The culture has been maintained using Bold's Basal Medium (BBM) (Orosa, Torres, Fidalgo, & Abalede, 2000) with half of the raceway pond culture being exchanged with fresh medium every 7 days. The pond has been operated for four years, and a stable algal population mainly containing green algae and cyanobacteria species has been established.

RAB system design and operation

The detailed RAB system design has been described in our previous publications (Gross et al., 2013, 2015; Gross & Wen, 2018). In brief, a flexible cotton duct canvas belt was stretched around drive shafts to form a vertical configuration. The lower region (~10%) of the belt was submerged in a liquid reservoir (1.2-L working volume) to supply nutrients, while the rest of the belt was exposed to the air to access light irradiation. The shafts were driven by a motor at speed of 4 cm/s to rotate the belt between the liquid and gas phases. To initiate cell attachment on the RAB belt, the liquid reservoir was inoculated with the algal seed culture and the RAB belt was rotated under continuous illumination of 110–120 μmol photons m^{-2} s^{-1} at 25°C. The suspended algal cells gradually attached on the RAB belt over a period of 2–3 weeks, during which the reservoir was supplemented with additional seed culture to compensate for water evaporative loss. After initial attachment, the algal biomass was harvested by scraping and the residual colonies remained on the material served as inoculum for the next growth cycle. During both the initial biofilm establishment stage and continuous culture stage, the biofilm was not thick enough to block the inner layer and no major "slough off" happened for the biofilm. However, there were still a small portion of suspended cells in the reservoir (<0.1 g/L).

Each wastewater stream was used as the influent to feed the RAB liquid reservoir, with the equal volume of the effluent being discharged. The effluent discharge/influent feeding was operated on daily basis at a rate of 1.2- and 0.4-L/day. Considering the reservoir volume of 1.2-L, these two feeding rates corresponded to 1 and 3 days of hydraulic retention time (HRT), respectively. These two HRT levels were commonly reported in previous report and can be potentially adopted by MWRD in their water resource recovery facility (Zhao, Kumar, Gross, Kunetz, & Wen, 2018). A sample of effluent (~25 ml) was used for subsequent analysis. The sample was centrifuged at 1,859 *g* at 4°C for 5 min to remove the solid residual (the suspended algal cells); it should be noted that the solid residues may contain precipitated salts. The supernatant was

immediately analyzed for TDS and chloride concentrations. The remaining supernatant was stored at −20°C for further analyzing salt concentrations. The biomass was harvested by scraping the biofilm from the RAB belt every 6 days. The harvested biomass was rinsed three times with distilled water and centrifuged at 1,859 *g* to remove the salts precipitated on the biofilm. The cell pellets were then freeze-dried to determine the cell dry weight and then stored for further analysis of ash and ions contents.

The algal growth in RAB reactors was evaluated using the biomass productivity based on both volume of the liquid reservoir ($P_{\text{volume-RAB}}$) and surface of the belt ($P_{\text{surface-RAB}}$), that is,

$$P_{\text{volume}-\text{RAB}} = \frac{W}{V}, \tag{1}$$

$$P_{\text{surface}-\text{RAB}} = \frac{W}{A \times F}, \tag{2}$$

where W is the dry weight (mg) of biomass harvested from the RAB belt, V is the volume of the liquid reservoir (1.2-L), A is the surface area of the attachment belt (0.171 m^2), and F is the frequency of harvesting biomass (6 days).

Bubble column design and operation

Bubble column (BC) reactor was also used in this work. As bubble column reactor is a typical suspension-based algal culture system, the TDS removal performance from this reactor will provide a comparison baseline to the biofilm-based RAB system. The BC reactors were made from Pyrex glass with an inner diameter of 6.5 cm and a height of 50 cm. Each column had a working volume of 1.2-L. The reactor was inoculated with 1.2-L seed cultures.

Unlike RAB reactor, the HRT of BC was only set at 3 days, that is, 400 ml of effluent was discharged from the reactor and same amount of influent was fed on daily basis. HRT = 1 day was not used for BC reactor as cell washout will happen at this HRT level. To establish the steady state of continuous culture in BC reactor, BBM was first used as influent to the reactor in the first 6 days; then, the feeding influents were switched to the different wastewaters as described in earlier. During the continuous operation, the samples of effluent discharged from the BCs were centrifuged to separate cell suspension into supernatant and biomass pellets. The supernatant was stored for analysis of TDS, chloride, and salt concentrations. The cell pellet was rinsed with distilled water and centrifuged at 1,859 *g* to remove the salts attached on the biofilm. This rinse step was repeated three times. The cell pellets were then freeze-dried to determine the cell dry weight and then stored for further analysis of ash and ion contents. The BCs were aerated with air at 1.0 L/min under continuous illumination of 110–120 μ m^{-2} s^{-1} light intensity at 25°C.

The volumetric biomass productivity in BCs (P_{BC}) was determined as follows:

$$P_{\text{volume}-\text{BC}} = \frac{C}{\text{HRT}}. \tag{3}$$

where C is the biomass concentration (mg/L, dry basis), and HRT is set at 3 days. The productivity based on both ash-containing and ash-free biomass was determined.

Determination of TDS, chloride, and other ion concentrations in liquid

Total dissolved solids and chloride concentrations were determined by Multi-Parameter PCSTesr 35 (Oakton, CA, USA) and Chloride Test Kits (Hach, CO, USA), respectively. The concentrations of the sodium, potassium, calcium, magnesium, and sulfur were determined by an iCAP 7400 inductively coupled plasma-optical emission spectrometry (ICP-OES; Thermo Scientific) with the program Qtegra (Version 2.7.2425.65; Thermo Scientific). Nitric acid (2%) was used as rinse solution. Yttrium ICP standard (5 ppm) and IV-ICPMS-71A (Inorganic, USA) were used as the internal standard and elemental standards, respectively. The wavelength for sodium, potassium, calcium, magnesium, and sulfur was 589, 766, 315, 279, and 180 nm, respectively. The wavelength was chosen based on EPA-METHOD 6010 C and the elemental standards.

Determination of ash and ion contents in biomass

The ash content of biomass was determined by heating the biomass at 550°C for 6 hr. To analyze the contents of various elements, 5 ml nitric acid was used to digest about 20 mg dry biomass in an Anton-Paar Multiwave GO system with a 30-min-long microwave program (10-min ramp to reach a power of 1,200 W, followed with 10 min at 1,200 W and 180°C and then 10-min cooling). Digested samples were diluted with deionized water into 50 ml, which were then analyzed for elemental composition using ICP-OES as described earlier. The biomass contents of these elements were calculated based on the element concentrations in the digested liquid and the biomass dry weight.

Determination of EPS compositions in algal biomass

The biomass harvested from the RAB and BC reactors were treated with sonication to extract EPS (Wang, Kuo-Dahab, Dolan, & Park, 2014). In brief, the cell pellet was suspended in 20 ml of phosphate buffer solution (10 mM NaCl, 1.2 mM KH_2PO_4, and 6 mM Na_2HPO_4) at a concentration equivalent to 1 g/L (dry basis). The cell pellet solution was placed in an ice bath, and EPS was extracted with a Model 500 Sonic Dismembrator (Fisher Scientific, USA) at 40% sonication intensity (20 kHZ) for 2 min. After treatment, the microscopic observation showed that algal cells remained intact, indicating no major cell lysis by the given condition of sonication. The samples were then centrifuged at 9,418 *g* for 15 min, and the supernatant containing EPS was collected. The protein and polysaccharide concentrations in the supernatant solution were determined based on the Coomassie blue method (Bradford, 1976) and colorimetric method (Dubois, Gilles, Hamilton, Rebers, & Smith, 1956), respectively. These concentrations (mg/L) were then converted into the EPS content of the protein and the polysaccharide (mg/g dry biomass) based on the volume of the supernatant

Table 2. Biomass productivity[a] and ash content of RAB at 1-day HRT (RAB-1), RAB at 3-day HRT (RAB-3), and bubble column at 3-day HRT (BC-3) fed with different wastewater sources

	ALGAL REACTORS AND HRT		
PARAMETERS	RAB-1	RAB-3	BC-3
P_{volume} (mg DW/L-day) (ash-containing[b])			
Industrial WW–low TDS	75 ± 1	85 ± 18	126 ± 17
Industrial WW–high TDS	363 ± 3	364 ± 43	304 ± 23
Ames WW	89 ± 20	85 ± 19	97 ± 15
Ames WW + NaCl	86 ± 19	79 ± 13	110 ± 16
$P_{surface}$ (mg DW/m^2-day) (ash-containing[b])			
Industrial WW–low TDS	527 ± 3	596 ± 127	—
Industrial WW–high TDS	2,549 ± 5	2,556 ± 300	—
Ames WW	623 ± 137	595 ± 131	—
Ames WW + NaCl	600 ± 130	553 ± 93	—
Ash content (%)			
Industrial WW–low TDS	31 ± 2	25 ± 7	31 ± 4
Industrial WW–high TDS	62 ± 11	52 ± 1	65 ± 1
Ames WW	20 ± 3	14 ± 5	23 ± 2
Ames WW + NaCl	22 ± 7	17 ± 5	15 ± 2
P_{volume} (mg AFDW/L -day) (ash-free[c])			
Industrial WW–low TDS	52 ± 1	64 ± 14	87 ± 12
Industrial WW–high TDS	139 ± 1	174 ± 20	106 ± 8
Ames WW	71 ± 16	73 ± 16	75 ± 11
Ames WW + NaCl	67 ± 14	65 ± 13	94 ± 14
$P_{surface}$ (mg AFDW/m^2-day) (ash-free [c])			
Industrial WW–low TDS	366 ± 2	446 ± 97	—
Industrial WW–high TDS	977 ± 4	1,219 ± 143	—
Ames WW	497 ± 109	511 ± 112	—
Ames WW + NaCl	471 ± 101	458 ± 93	—

[a]RAB biomass productivity was based on both reservoir volume (P_{volume}) and belt surface ($P_{surface}$). BC biomass productivity was based on volume (P_{volume}).

[b]Ash-containing biomass refers to "as-is" biomass harvested from the RAB system after rinse.

[c]Ash-free biomass was the "ash-containing biomass" excluding ash portion.

and the equivalent biomass dry weight. Total EPS content was determined by combining the protein and polysaccharide contents.

Statistical analysis

The significance of differences among mean values was determined using analysis of variance (one-way ANOVA), followed by Tukey's multiple range test. A significance level of $p < 0.05$ was considered significant. For each experimental condition, three replicates were performed. Data were presented as the mean values with standard deviations of the three replicates.

Results and Discussion

Microalgal growth and EPS content in RAB and bubble column reactors

The algal growth in RAB and bubble column (BC) reactors was evaluated based on the biomass productivity as described in Equations 1–3, respectively. As shown in Table 2, for each type of wastewater stream, the volumetric (ash-containing) biomass productivity (P_{volume}) of RAB and BC was within a similar range. Between the two HRT levels of the RAB reactor, the surface-based (ash-containing) biomass productivity did not vary significantly ($p > 0.05$). Among four different wastewaters, industrial WW–high TDS resulted in 3–5 times higher (ash-containing) biomass productivity than those fed with other types of wastewaters. Adding sodium chloride (NaCl) to the real wastewater (Ames WW) at the level of 1 g/L did not have a significant ($p > 0.05$) impact on the cell growth, indicating the tolerance of algae at this level of salinity.

Table 2 also shows that for both RAB and BC cultures, the ash content of the biomass derived from the industrial WW–high TDS was the highest level due to the high salt concentration in this type of wastewater. For the ash-free biomass, the industrial WW–high TDS still resulted in the 1–2 times higher biomass productivities than the other three types of wastewaters although this difference was as drastic as the ash-containing biomass.

The above trends of cell growth were probably due to the different nutrient levels provided by the wastewater. It was found that the effluent nitrogen of the RAB reactors during the continuous operation reached to almost zero (<0.1 mg/L). Considering the nitrogen profile for the four types of wastewater (Table 1), it indicates the RAB reactor fed with industrial WW-high TDS consumed the most nitrogen, while the other three wastewater streams had similar nitrogen levels. This nitrogen consumption correlated well with the cell growth of these four reactors (Table 2).

In addition to cell growth, the algal biomass was further characterized for the EPS content. In algal reactor, particularly the biofilm systems, microalgae cells excrete EPS into their immediate environment to form a hydrated biofilm matrix (Gross et al., 2016), which was believed to help to adsorb TDS from wastewater. As shown in Figure 1, throughout all the biomass samples the polysaccharide content was much higher than the proteins. The EPS protein contents in RAB and BC biomass were similar, while the EPS polysaccharide was higher in RAB-derived biomass than those in BC biomass, and as a result, RAB biomass contained a higher total EPS than the BC

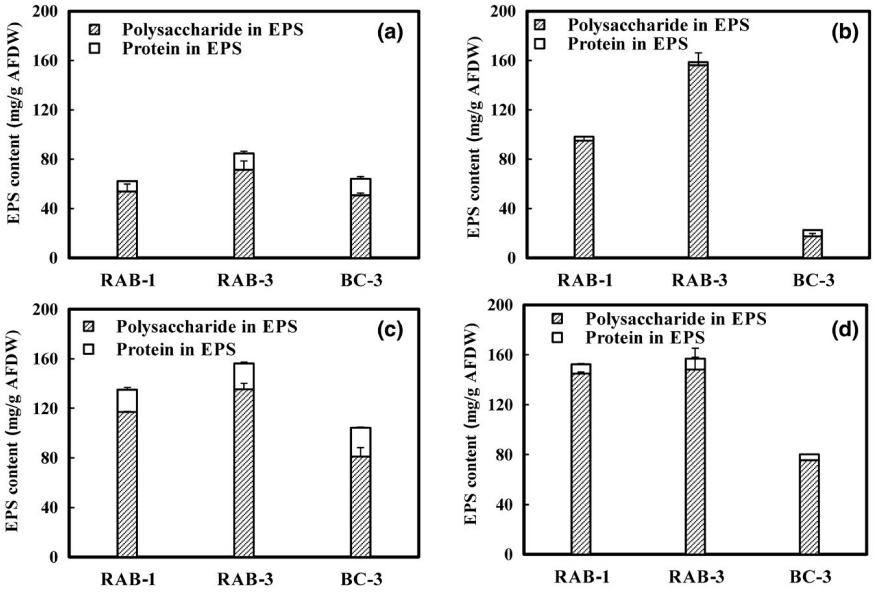

Figure 1. The contents of polysaccharide and protein in EPS of algal biomass (ash-free dry weight, AFDW) produced from RAB at 1-day HRT (RAB-1), RAB at 3-day HRT (RAB-3), and bubble column at 3-day HRT (BC-3). The influents feeding to the reactors were WW–low TDS (a); industrial WW–high TDS (b); Ames WW (c); and Ames WW + NaCl (d).

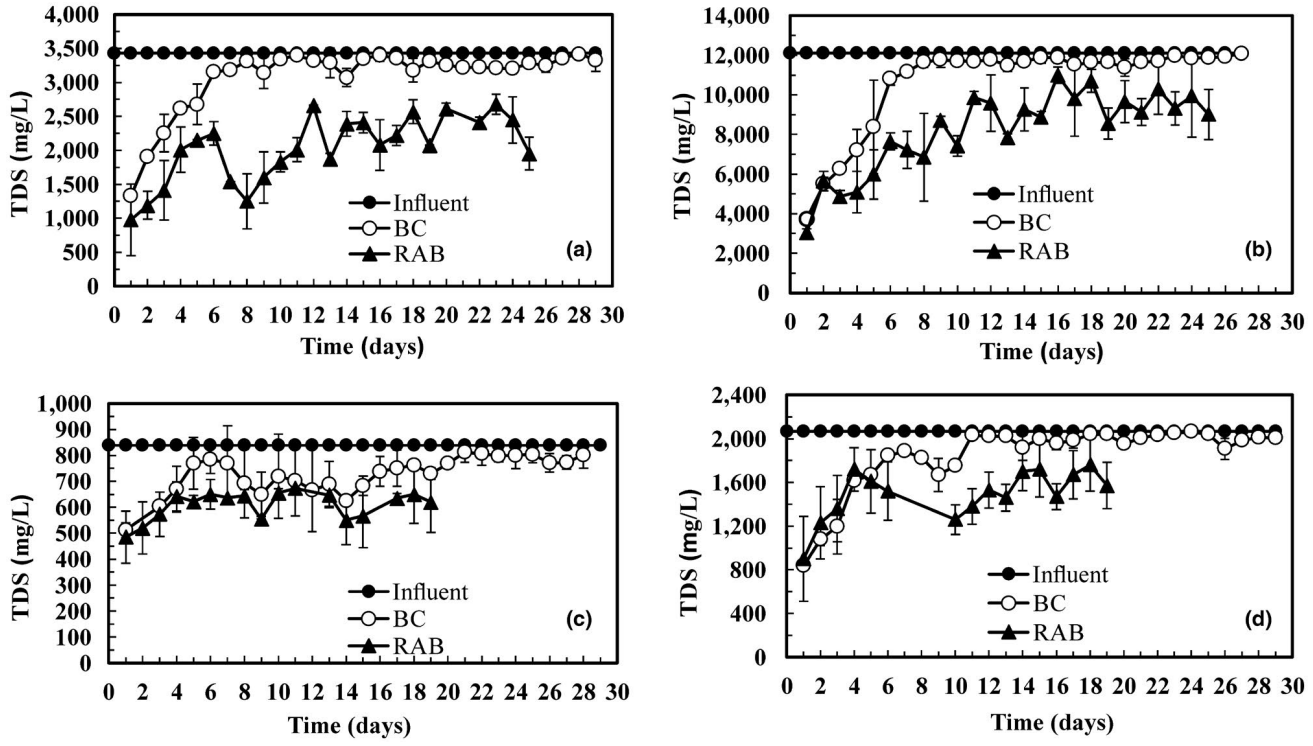

Figure 2. The concentration of TDS in the influent and effluent during the continuous operation (HRT = 3 days) of the RAB and BC reactors. The influents feeding to the reactors were industrial WW–low TDS (a); industrial WW–high TDS (b); Ames WW (c); and Ames WW + NaCl (d).

biomass. Between the two HRT levels in the RAB reactors, the 3-day HRT resulted in a higher EPS polysaccharide than the 1-day HRT (Figure 1).

Polysaccharides and proteins are two major components in algal EPS (Xiao & Zheng, 2016). Polysaccharide protects cells from unfavorable stress and is involved in cell-to-cell interactions, adhesion, and biofilm formation (Liu, Pohnert, & Wei, 2016). In the present study, the accumulation of EPS polysaccharide was much higher than the EPS proteins in all algal biomass. This was probably due to the nitrogen deficiency in the wastewater leading

to low protein synthesis. Instead, cells tended to accumulate carbon reserve compounds such as polysaccharides (Díaz Bayona & Garces, 2014). The polysaccharide accumulation also depends on the cell growth. A higher biomass productivity in the RAB systems resulted in a higher polysaccharide level compare to the BC system. The longer HRT also resulted in a better cell growth and thus a higher EPS polysaccharide level.

TDS removal performance

The TDS concentrations in the effluent of RAB and BC reactors were monitored during the entire operation period. Figure 2 shows the TDS concentrations in influent and effluent of RAB and BC reactors at 3-day HRT. For each type of wastewater, the influent TDS of the RAB and BC reactors was maintained at a constant level. The effluent TDS increased initially and reached the steady state with the culture progressing. It should be noted that at the first 8–10 days, the low levels of TDS in the reactor effluents was mainly caused by the "dilution" effect, that is, the influent TDS was diluted by the BBM medium that was used for the initial cell growth. During this period (8–10 days), the cells were still in the transitional stage. With the continuous culture progressing, the reactors gradually reached equilibrium and the effluent TDS reached to steady-state concentration. These steady-state concentrations were the "true" concentrations reflecting the TDS removal capacity by the algal reactors (Figure 2).

Based on the steady-state TDS concentrations, a comprehensive summary of the TDS removal performance in RAB and BC reactors is presented (Table 3). Overall, TDS removal efficiency (TDS-E) of the RAB reactors was higher than the BC reactors. Among the two HRT levels for the RAB reactors, the longer HRT resulted in higher TDS-E values. Among four types of wastewaters, industrial WW–high TDS led in the highest TDS-E. The Ames WW + NaCl had a lower removal efficiency.

Total dissolved solids removal rate by the algal culture systems was evaluated based on the liquid volume (TDS-R_{volume}) and attachment surface (TDS-$R_{surface}$). Similar to the trend of TDS-E, TDS-R_{volume} of the RAB reactors was much higher than that of the BC reactor (Table 3). The industrial WW–high TDS also demonstrated the best TDS removal rate among four wastewaters. However, the Ames WW + NaCl had a higher removal rate due to the high input of NaCl from the influent. However, contrary to the trend of TDS-E with HRT, shorter HRT resulted in a higher TDS-R_{volume} and TDS-$R_{surface}$ values for the RAB reactors (Table 3), probably due to the higher TDS mass turnover rate at shorter HRT.

The use of microalgae for TDS removal has been widely reported in the suspension-based cultivation systems. For example, El-Bestawy (2008) reported that the alga *Tolypothrix ceylonica* reduced TDS by 14% in mixed domestic/industrial wastewater. Maity et al. (2014) found that the green alga *Leptolyngbya* sp. JPMTW1 removed 13% TDS from wastewater. Renuka, Sood, Ratha, et al. (2013) found that an algae consortium reduced TDS by 28% (from 1,120 to 806 mg/L). More than 50% reduction of TDS from mixed industrial wastewaters was reported with the consortium of *Chlorella* and *Phormidium* after 20 days of incubation (Das, Ramaiah, Pereira, & Naseera, 2018), while even higher TDS removal efficiency (65%–80%) was reported in industrial wastewaters (Khan et al., 2017), oil and gas production wastewater (Lutzu & Dunford, 2019), and distiller wastewater (Krishnamoorthy et al., 2019). From a percentage perspective, the TDS removal efficiency reported in this work (TDS-E [%], Table 3), particularly for the BC reactor, was in the lower end compared to the date reported in previous research. However, those previous studies were based on batch culture with 7–30 days of culture time. In this work, the BC and RAB reactors were based on the continuous culture resulting in a much higher volumetric removal rate (i.e., TDS-R_{volume} [mg/L-day],

Table 3. TDS removal efficiency (TDS-E, %), removal rate based on liquid volume (TDS-R_{volume}, mg/L-day), and removal rate based on surface area (TDS-$R_{surface}$, mg/m^2-day) of RAB reactor at 1-day HRT (RAB-1), RAB rector at 3-day HRT (RAB-3), and bubble column reactor at 3-day HRT (BC-3), respectively, fed with different wastewater sources

TDS REMOVAL PARAMETERS UNDER DIFFERENT WW SOURCES	ALGAL REACTORS AND HRT		
	RAB-1	RAB-3	BC-3
TDS-E (%)			
Industrial WW–Low TDS	9 ± 3	16 ± 5	4 ± 0
Industrial WW–high TDS	24 ± 4	27 ± 3	3 ± 1
Ames WW	12 ± 1	26 ± 4	8 ± 2
Ames WW + NaCl	8 ± 1	14 ± 5	3 ± 1
TDS-R_{volume} (mg/L-day)			
Industrial WW–Low TDS	309 ± 38	183 ± 13	46 ± 2
Industrial WW–High TDS	2,783 ± 192	1,089 ± 189	121 ± 11
Ames WW	101 ± 13	73 ± 14	22 ± 3
Ames WW + NaCl	165 ± 17	96 ± 15	21 ± 4
TDS-$R_{surface}$ (mg/m^2-day)			
Industrial WW–Low TDS	2,166 ± 174	1,284 ± 100	—
Industrial WW–High TDS	19,530 ± 1,479	7,642 ± 52	—
Ames WW	707 ± 90	511 ± 77	—
Ames WW + NaCl	1,159 ± 185	676 ± 72	—

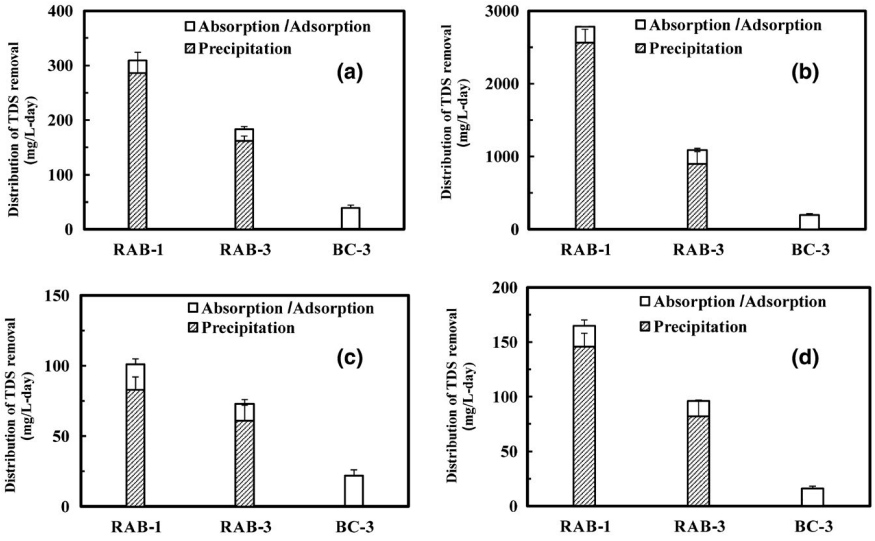

Figure 3. The distribution of TDS removal by chemical precipitation, EPS-based adsorption, and cell-based absorption from RAB at 1-day HRT (RAB-1), RAB at 3-day HRT (RAB-3), and bubble column at 3-day HRT (BC-3). The influents feeding to the reactors were WW–low TDS (a); industrial WW–high TDS (b); Ames WW (c); and Ames WW + NaCl (d).

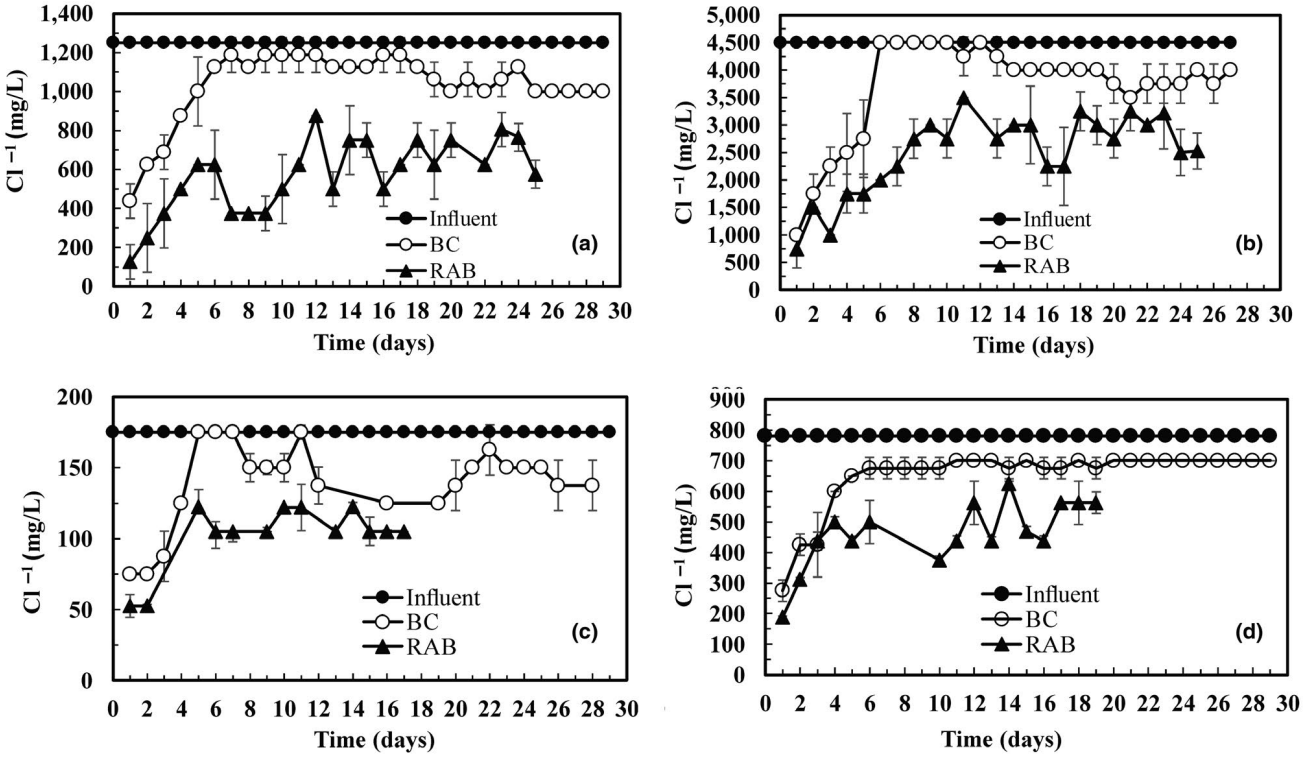

Figure 4. The concentration of chloride in the influent and effluent during the continuous operation (HRT = 3 days) of the RAB and BC reactors. The influents feeding to the reactors were industrial WW–low TDS (a); industrial WW–high TDS (b); Ames WW (c); and Ames WW + NaCl (d).

Table 3). For example, the BC reactor removed TDS at a rate of 21–121 mg/L-day (Table 3) and the RAB system removed at 101–2,783 mg/L-day, while the TDS removal rates of the previous reports were calculated as 9 mg/L-day (Maity et al., 2014), 25 mg/L-day (El-Bestawy, 2008), 45 mg/L-day (Renuka, Sood, Ratha, et al., 2013), 130 mg/L-day (Das et al., 2018), 349 mg/L-day (Lutzu & Dunford, 2019), 9–30 mg/L-day (Khan et al., 2017), and 4 mg/L-day (Krishnamoorthy et al., 2019). With the further process optimization such as light intensity, TDS removal efficiency by the RAB and BC reactors can be further increased.

Table 4. Chloride removal efficiency (Chloride-E, %), removal rate based on liquid volume (Chloride-R_{volume}, mg/L-day), and removal rate based on surface area (Chloride-$R_{surface}$, mg/m^2-day) of RAB reactor at 1-day HRT (RAB-1), RAB rector at 3-day HRT (RAB-3), and bubble column reactor at 3-day HRT (BC-3), respectively, fed with different wastewater sources

CHLORIDE REMOVAL PARAMETERS UNDER DIFFERENT WW SOURCES	ALGAL REACTORS AND HRT		
	RAB-1	RAB-3	BC-3
Chloride-E (%)			
Industrial WW–Low TDS	21 ± 3	32 ± 2	13 ± 3
Industrial WW–High TDS	27 ± 4	37 ± 3	13 ± 2
Ames WW	15 ± 1	34 ± 5	20 ± 2
Ames WW + NaCl	16 ± 3	35 ± 5	11 ± 1
Chloride-R_{volume} (mg/L-day)			
Industrial WW–Low TDS	262 ± 25	133 ± 14	54 ± 4
Industrial WW–High TDS	1,215 ± 310	555 ± 63	195 ± 14
Ames WW	26 ± 4	20 ± 3	11 ± 3
Ames WW + NaCl	112 ± 17	93 ± 8	29 ± 1
Chloride-$R_{surface}$ (mg/m^2-day)			
Industrial WW–Low TDS	1,842 ± 174	936 ± 90	—
Industrial WW–High TDS	8,526 ± 292	3,895 ± 414	—
Ames WW	184 ± 20	139 ± 10	—
Ames WW + NaCl	786 ± 60	650 ± 70	—

The mechanisms of TDS removal by RAB and BC reactors

The above results indicate that in RAB reactors, the TDS removal rate (Table 3) was much higher than the biomass productivity (Table 2). For example, the volumetric TDS removal (TDS-R_{volume}) of RAB-1 was 309 ± 38 mg/L-day, while the volumetric biomass productivity (P_{volume}) of the same reactor was only 75 ± 1 mg DW/L-day for ash-containing biomass and 52 ± 1 mg AFDW/L-day for ash-free biomass. Similar trends were also observed for other wastewater streams among RAB reactors. This drastic difference between the TDS removal and cell growth was considered due to the precipitation of TDS salt on the RAB biofilm. As a matter of fact, during the experiments, we observed a significant amount of salts precipitated on the surface of the

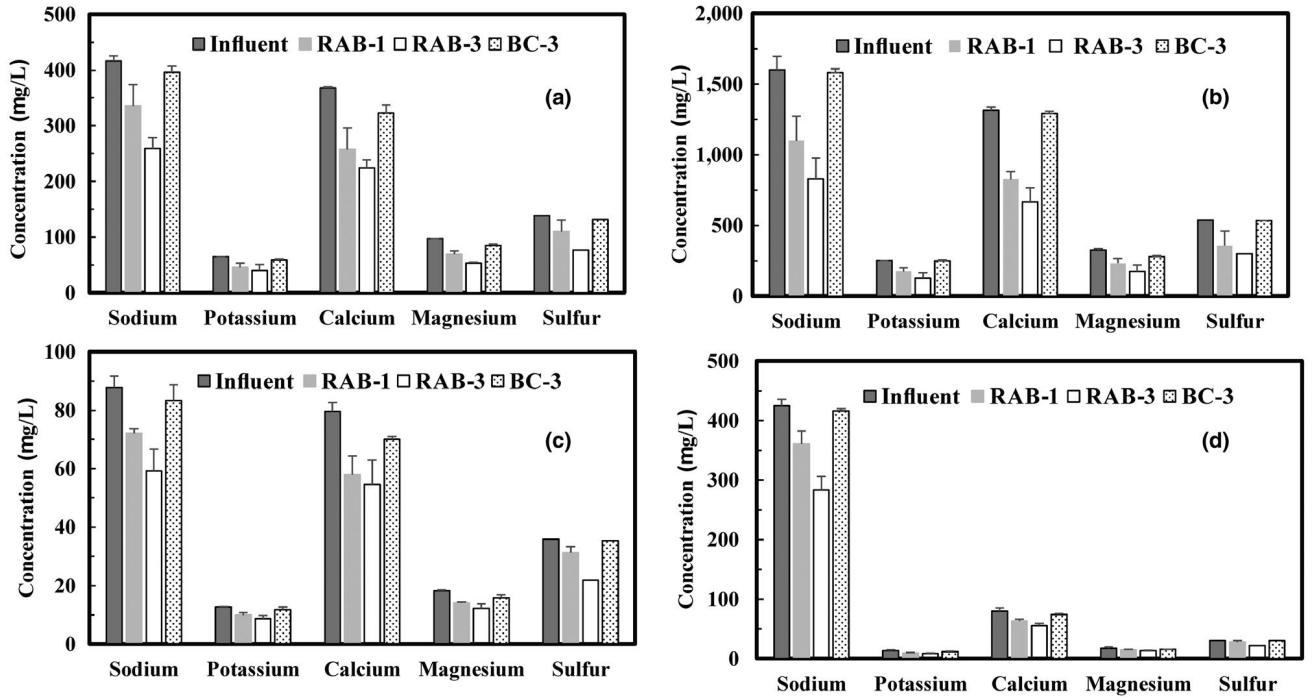

Figure 5. Sodium, potassium, calcium, magnesium, and sulfur concentrations in the influent and effluent of the continuous operation of RAB and BC reactors. The influents feeding to the reactors were industrial WW–low TDS (a); industrial WW–high TDS (b); Ames WW (c); and Ames WW + NaCl (d). The RAB reactor was operated at 1-day HRT (RAB-1) and 3-day HRT (RAB-3); the bubble column reactor was operated at 3-day HRT (BC-3). The data were reported at the steady state of the reactors.

Table 5. Ion contents of algal biomass (ash-containing) produced from RAB at 1-day HRT (RAB-1) and RAB at 3-day HRT (RAB-3) and bubble column at 3-day HRT (BC-3) fed with different wastewater sources

	ALGAL REACTORS AND HRT		
COMPOSITIONS	RAB-1	RAB-3	BC-3
Industrial WW–low TDS			
Sodium (%)	0.98 ± 0.23	0.77 ± 0.18	0.68 ± 0.07
Potassium (%)	0.68 ± 0.05	0.70 ± 0.02	0.74 ± 0.05
Calcium (%)	6.60 ± 0.27	5.34 ± 0.07	5.65 ± 0.15
Magnesium (%)	1.34 ± 0.23	0.86 ± 0.00	2.37 ± 0.04
Sulfur (%)	1.48 ± 0.16	0.88 ± 0.17	0.74 ± 0.05
Industrial WW–high TDS			
Sodium (%)	2.56 ± 0.16	2.43 ± 0.04	1.61 ± 0.04
Potassium (%)	0.60 ± 0.12	0.72 ± 0.01	0.68 ± 0.00
Calcium (%)	13.54 ± 1.82	12.35 ± 0.59	9.90 ± 0.36
Magnesium (%)	3.08 ± 0.25	2.02 ± 0.25	7.33 ± 0.20
Sulfur (%)	5.81 ± 0.30	4.57 ± 0.17	0.48 ± 0.00
Ames WW			
Sodium (%)	0.26 ± 0.05	0.26 ± 0.01	0.15 ± 0.03
Potassium (%)	0.69 ± 0.08	0.68 ± 0.08	0.70 ± 0.24
Calcium (%)	3.67 ± 0.00	3.76 ± 0.00	5.38 ± 0.67
Magnesium (%)	0.43 ± 0.10	0.38 ± 0.02	0.45 ± 0.11
Sulfur (%)	0.75 ± 0.05	0.72 ± 0.07	0.84 ± 0.07
Ames WW + NaCl			
Sodium (%)	1.06 ± 0.25	0.79 ± 0.06	0.73 ± 0.09
Potassium (%)	0.67 ± 0.10	0.75 ± 0.04	0.77 ± 0.00
Calcium (%)	6.92 ± 0.00	4.41 ± 0.00	5.72 ± 0.09
Magnesium (%)	0.31 ± 0.10	0.51 ± 0.20	0.31 ± 0.00
Sulfur (%)	0.69 ± 0.02	0.64 ± 0.02	0.85 ± 0.08

RAB biofilm and removed from the system with the harvested RAB biofilm. As these abiotic precipitated salts were actually not contributing to the cell growth, they were rinsed out and not accounted when the cell growth was measured.

However, from TDS removal perspective, the precipitation played an important role to remove TDS from the RAB system. The precipitation has been reported as one mechanism for TDS removal in other research (Malik, 2004; Silva, Cadorin, & Rubio, 2010). In addition to precipitation, EPS-based adsorption and the cellular absorption are another two mechanisms for TDS removal. In this work, those adsorption- and absorption-based TDS was calculated by subtracting ash-free biomass from ash-containing biomass. The contribution of precipitation on TDS removal can be estimated by subtracting the adsorption- and absorption-based TDS from the total TDS removed (TDS-R_{volume}, Table 3). Using the above approaches, the relative contribution of precipitation, and adsorption/absorption to the TDS removal is presented in Figure 3. As shown in the figure, the precipitation played a major role in of the TDS removed for the RAB reactors. For the BC reactors, all the TDS removal was through the adsorption/absorption.

Chloride removal performance

As chloride is the major ion in all the four wastewaters tested (Table 1), the removal performance of this specific TDS species was investigated. Similar to the trends of TDS (Figure 2), Figure 4 shows that the effluent chloride was low initially as the culture was in transition from low chloride medium (BBM medium) to the experimental wastewater streams. Depending on the types of the wastewater and reactors, the effluent chloride concentrations reached steady state in 10–20 days.

The chloride removal performance is summarized in Table 4. Overall, the trends of the chloride removal efficiency and removal rate were similar to those observed in the TDS. Both chloride removal efficiency and removal rate (volume- and surface-based) of the RAB reactors were higher than those of the BC reactor. Among the two HRT levels, shorter HRT resulted in a lower chloride removal efficiency but much higher removal rate. Industrial WW–high TDS had the best chloride removal performance than the other three types of wastewaters. The above trends of chloride removal among reactors and the influent streams were also due to the different salt removal mechanisms discussed earlier, that is, the chemical precipitation was considered the major mechanism in the chloride removal by the RAB reactor.

It should also be noted that the microalgae may adapt to the high chloride concentration. For example, industrial WW-high TDS (thus high chloride) resulted in a higher algae growth, while Ames WW + NaCl resulted in a similar growth performance as the Ames WW (Table 2).

The adaptation to high chloride level has been reported in green alga *Botryococcus braunii* (Rao, Dayananda, Sarada, Shamala, & Ravishankar, 2007). Ramírez, Vélez, Rendón, and Alzate (2018) reported the use of algae in the bioremediation of water where chloride removal efficiencies ranged within 16%–40% with different species at an initial chloride concentration of 20 g/L.

Removal of various ions from wastewater

In addition to chloride, the removal of other major ionic components such as sodium, potassium, calcium, magnesium, and sulfur (Table 1) from wastewaters was also determined. The concentration of these metal and non-metal ions in the influent and effluent (at steady state) was evaluated. As shown in Figure 5, among various ions, sodium and calcium were predominant, followed with sulfur, magnesium, and potassium. The RAB reactors demonstrated ion removal capacities for all the wastewaters used. The RAB reactors at 3-day HRT (RAB-3) removed more ions than those at 1-day HRT (RAB-1) (Figure 5). When industrial WW–high TDS was used as the influent, RAB reactor removed ~50% (3-day HRT) and ~30% (1-day HRT) of these five ions from the influent, while only ~2% of these five ions was removed from the BC reactors (Figure 5b). The industrial WW–high TDS (Figure 5b) also led to the highest removal efficiency of the ions compared to other three wastewaters (Figure 5a,c,d). On the contrary, for the BC reactor, the influent and effluent concentrations of various ions were almost the same (Figure 5), indicating the BC reactors had a limited capability of removing those elements.

The removal of different ion species in algal culture may be due to the cation transport through the cell membrane, adsorption, and chemical precipitation (Malik, 2004). Algae have been reported notable capabilities of removing ions such as sodium, calcium, magnesium, potassium, and sulfur through biosorption (Wang et al., 2014; Zhou, Sheng, Zhao, Gross, & Wen, 2018). Zhou, Min, et al. (2012) reported 92% removal of calcium, and 20% removal of sodium, potassium, and sulfur through bio-assimilation and precipitation. In this work, the RAB reactors demonstrated a high performance of removing these metals and non-metal ions, especially for the industrial WW–high TDS. This was due to the multiple mechanism particularly through chemical precipitation. For example, the pH of initial wastewaters was at alkaline range (Table 1). The pH of the wastewaters increases to an even higher levels (data not shown). This alkaline pH may facilitate precipitation of the ions. The impact of high pH on the phosphate precipitation has been reported (Song, Hahn, & Hoffmann, 2002). Zhou, Min, et al. (2012) also reported that calcium concentration dropped drastically when the pH exceeded 9 after 4 days of algal cultivation in municipal wastewater.

Ion contents of algal biomass

The biomass harvested from the algal reactors was analyzed for its ion content. As shown in Table 5, calcium was the most predominant ion in the biomass followed with sulfur, magnesium, sodium, and potassium. Potassium content in biomass maintained at a relatively constant level (0.6%–0.7%) throughout all the experimental conditions, while calcium, magnesium, sodium, and sulfur contents were altered and matched with the concentration level of these ions in wastewaters.

It is well known that algae have the notable biosorption ability for metal ions such as calcium, magnesium, sodium, and potassium, due to the negatively charged function groups on the cell surface and the ion-specific or ion group-specific sites of carriers (Ayangbenro & Babalola, 2017). Sodium and potassium adjust electro-neutrality and osmotic equilibrium of algae intracellular and extracellular environment to maintain the appropriate functions in algal cells (Wang et al., 2014). Potassium is also the component of many proteins and enzymes required for biochemical reactions. Higher plants can actively absorb potassium and regulate absorption rate to maintain the internal stability by keeping potassium at a relatively narrow level (Schachtman & Schroeder, 1994); in this work, the stable potassium content across different biomass samples indicated algal cells may have the similar capability of adjusting potassium adsorption to maintain a balanced intracellular and extracellular osmosis (Wang et al., 2014). As for sulfur content, the results from sulfur removal from different wastewaters (Figure 5) and sulfur accumulation in biomass (Table 5) indicate that biofilm algae in RAB reactors can absorb more sulfur than the suspended algae in BC reactors. The superior capability of assimilating sulfur by the RAB algae was probably due to the physical adsorption by the EPS (Kesaano & Sims, 2014; Zhou et al., 2018).

It should be noted that the data reported here are based on ash-containing biomass, that is, the precipitated ions have been washed; thus, the ions accumulated in the biomass are through adsorption/absorption. The EPS in the RAB biomass were considered the one major contributor for adsorbing TDS ions. When used to treat wastewater with high content of TDS, the various functional groups in polysaccharides such as carboxyl and hydroxyl groups adsorb those inorganic and organic matters (Flemming & Leis, 2002) and, therefore, resulted in very high binding capacity (Guibaud & van Hullebusch, 2006; Guibaud, Tixier, Bouju, & Baudu, 2003). The binding between EPS and divalent cations such as Ca^{2+} and Mg^{2+} has also been reported as the main mechanism in maintaining the microbial aggregate structure (Mayer et al., 1999).

Conclusion

This work demonstrates that the feasibility of using RAB reactors as a sustainable and environmentally friendly method can efficiently remove TDS from wastewaters. Depending on the HRT and type of wastewaters, the efficiencies of removing TDS, chloride, and ions of the RAB reactors were higher than the suspended algal culture system. The precipitation, EPS-based adsorption, and cellular absorption all contributed to the TDS removal from the RAB reactor, and precipitation was the major contributor. While in the suspended culture

systems, adsorption and absorption play the major role for TDS removal. In order to implement the system at a commercial scale, the operational parameters of the RAB system need to be optimized together with a thorough cost analysis.

Acknowledgments

This project was funded by Metropolitan Water Reclamation District of Greater Chicago (Grant #: 14-062-AP). The authors also like to thank Xuefei Zhao, Si Chen, Haoyuan Zhou (Iowa State University, USA), and Dr Jianping Yuan (Yat-Sen University, China) for their help during the project period. M. Gross and Z. Wen have equity interests in Gross-Wen Technologies, Inc., a company that may potentially benefit from the research results, and also serve on the company's Scientific Advisory Board. The terms of this arrangement have been reviewed and approved by Iowa State University in accordance with its conflict of interest policies.

Data Availability Statement

The data that support the findings of this study are available from the corresponding author upon reasonable request.

References

Ayangbenro, A. S., & Babalola, O. O. (2017). A new strategy for heavy metal polluted environments: A review of microbial biosorbents. *International Journal of Environmental Research and Public Health*, *14*(1), 94. https://doi.org/10.3390/ijerph14010094

Bradford, M. M. (1976). A rapid and sensitive method for the quantitation of microgram quantities of protein utilizing the principle of protein-dye binding. *Analytical Biochemistry*, *72*(1–2), 248–254. https://doi.org/10.1016/0003-2697(76)90527-3

Brix, K. V., Gerdesa, R., Curryc, N., Kaspera, A., & Grosella, M. (2010). The effects of total dissolved solids on egg fertilization and water hardening in two salmonids – Arctic Grayling (*Thymallus arcticus*) and Dolly Varden (*Salvelinus malma*). *Aquatic Toxicology*, *97*, 109–115. https://doi.org/10.1016/j.aquatox.2009.12.011

Canedo-Arguelles, M., Kefford, B. J., Piscart, C., Prat, N., Schafer, R. B., & Schulz, C. (2013). Salinization of rivers: An urgent ecological issue. *Environmental Pollution*, *173*, 157–167.

Chapman, P. M., Bailey, H., & Canaria, E. (2000). Toxicity of total dissolved solids associated with two mine effluent to chironomid larvae and early life stages of rainbow trout. *Environmental Toxicology and Chemistry*, *19*, 210–214.

Cho, S., Luong, T. T., Lee, D., Oh, Y., & Lee, T. (2011). Reuse of effluent water from a municipal wastewater treatment plant in microalgae cultivation for biofuel production. *Bioresource Technology*, *102*, 8639–8645. https://doi.org/10.1016/j.biortech.2011.03.037

Choudhary, P., Prajapati, S. K., Kumar, P., Malik, A., & Pant, K. K. (2017). Development and performance evaluation of an algal biofilm reactor for treatment of multiple wastewaters and characterization of biomass for diverse applications. *Bioresource Technology*, *224*, 276–284. https://doi.org/10.1016/j.biortech.2016.10.078

Das, C., Ramaiah, N., Pereira, E., & Naseera, K. (2018). Efficient bioremediation of tannery wastewater by monostrains and consortium of marine *Chlorella* sp and *Phormidium* sp. *International Journal of Phytoremediation*, *20*(3), 284–292.

Davis, R., Aden, A., & Pienkos, P. (2011). Techno-economic analysis of autotrophic microalgae for fuel production. *Applied Energy*, *88*, 3524–3531. https://doi.org/10.1016/j.apenergy.2011.04.018

Delattre, C., Pierre, G., Laroche, C., & Michaud, P. (2016). Production, extraction and characterization of microalgal and cyanobacterial exopolysaccharides. *Biotechnology Advances*, *34*, 1159–1179. https://doi.org/10.1016/j.biotechadv.2016.08.001

Díaz Bayona, K. C., & Garces, L. A. (2014). Effect of different media on exopolysaccharide and biomass production by the green microalgae *Botryococcus braunii*. *Journal of Applied Phycology*, *26*, 2087–2095.

Dubois, M., Gilles, K. A., Hamilton, J. K., Rebers, P. A., & Smith, F. (1956). Colorimetric method for determination of sugars and related substances. *Analytical Chemistry*, *28*, 350–356.

El-Bestawy, E. (2008). Treatment of mixed domestic-industrial wastewater using cyanobacteria. *Journal of Industrial Microbiology Biotechnology*, *35*, 1503–1516. https://doi.org/10.1007/s10295-008-0452-4

Flemming, H. C., & Leis, A. (2002). Sorption properties of biofilms. In H. C. Flemming, & G. Bitton (Eds.), *Encyclopedia of environmental microbiology* (Vol. *5*, pp. 2958–2967). New York, NY: Wiley-Interscience.

Gross, M., Henry, W., Michael, C., & Wen, Z. (2013). Development of a rotating algal biofilm growth system for attached microalgae growth with *in-situ* biomass harvest. *Bioresource Technology*, *150*, 195–201. https://doi.org/10.1016/j.biortech.2013.10.016

Gross, M., Mascarenhas, V., & Wen, Z. (2015). Evaluating algal growth performance and water use efficiency of pilot-scale revolving algal biofilm (RAB) culture systems. *Biotechnology and Bioengineering*, *112*, 2040–2050. https://doi.org/10.1002/bit.25618

Gross, M., & Wen, Z. (2018). *Revolving algal biofilm photobioreactor systems and methods*, US Patents #9,932,549 and #10,125,341.

Gross, M., Zhao, X., Mascarenhas, V., & Wen, Z. (2016). Effects of the surface physicochemical properties and the surface textures on the initial colonization and the attached growth in algal biofilm. *Biotechnology for Biofuels*, *9*(1), 38. https://doi.org/10.1186/s13068-016-0451-z

Guibaud, G., Tixier, N., Bouju, A., & Baudu, M. (2003). Relation between extracellular polymer's composition and its ability to complex Cd, Cu, and Pb. *Chemosphere*, *52*, 1701–1710. https://doi.org/10.1016/S0045-6535(03)00355-2

Guibaud, G., & van Hullebusch, E. F. (2006). Lead and cadmium biosorption by extracellular polymeric substances (EPS) extracted from activated sludges: pH-sorption edge tests and mathematical equilibrium modeling. *Chemosphere*, *64*, 1955–1962.

Iowa DNR. (2009). *Water quality standards review: chloride, sulfate and total dissolved solids*. Iowa Department of Natural Resources Consultation Package. Retrieved from http://www.iowadnr.gov/portals/idnr/uploads/water/standards/ws_review.pdf

Kennedy, A. J., Cherry, D. S., & Currie, R. J. (2003). Field and laboratory assessment of a coal-processing effluent in the Leading Creek Watershed, Meigs Co., Ohio. *Archievs of Environmental Contamination and Toxicology*, *44*, 324–331.

Kesaano, M., & Sims, R. C. (2014). Algal biofilm based technology for wastewater treatment. *Algal Research*, *5*, 231–240. https://doi.org/10.1016/j.algal.2014.02.003

Khan, S., Shamshad, I., Waqas, M., Nawab, J., & Ming, L. (2017). Remediating industrial wastewater containing potentially toxic elements with four freshwater algae. *Ecological Engineering*, *102*, 536–541. https://doi.org/10.1016/j.ecoleng.2017.02.038

Krishnamoorthy, S., Manickam, P., & Muthukaruppan, V. (2019). Evaluation of distillery wastewater treatability in a customized photobioreactor using blue-green microalgae-Laboratory and outdoor study. *Journal of Environmental Management*, *234*, 412–423. https://doi.org/10.1016/j.jenvman.2019.01.014

Kumar, P., Prajapati, S. K., Malik, A., & Vijay, V. K. (2017). Cultivation of native algal consortium in semi-continuous pilot scale raceway pond for greywater treatment coupled with potential methane production. *Journal of Environmental Chemical Engineering*, *5*(6), 5581–5587. https://doi.org/10.1016/j.jece.2017.10.044

Liu, L., Pohnert, G., & Wei, D. (2016). Extracellular metabolites from industrial microalgae and their biotechnological potential. *Marine Drugs*, *14*, 191–210. https://doi.org/10.3390/md14100191

Lutzu, G. A., & Dunford, N. T. (2019). Algal treatment of wastewater generated during oil and gas production using hydraulic fracturing technology. *Environmental Technology*, *40*, 1027–1034. https://doi.org/10.1080/09593330.2017.1415983

Maity, J. P., Hou, C. P., Majumder, D., Bundschuh, J., Kulp, T. R., Chen, C. Y., … Chen, C. C. (2014). The production of biofuel and bioelectricity associated with wastewater treatment by green algae. *Energy*, *78*, 94–103. https://doi.org/10.1016/j.energy.2014.06.023

Malik, A. (2004). Metal bioremediation through growing cells. *Environment International*, *30*, 261–278. https://doi.org/10.1016/j.envint.2003.08.001

Mayer, C., Moritz, R., Kirschner, C., Borchard, W., Maibaum, R., Wingender, J., & Flemming, H. C. (1999). The role of intermolecular interactions: Studies on model systems for bacterial biofilms. *International Journal of Biological Macromolecules*, *26*, 3–16. https://doi.org/10.1016/S0141-8130(99)00057-4

Orosa, M., Torres, E., Fidalgo, P., & Abalede, J. (2000). Production and analysis of secondary carotenoids in green alga. *Journal of Applied Phycology*, *12*, 553–556.

Pinto, P. X., Al-Abed, S. R., Balz, D. A., Butler, B. A., Landy, R. B., & Smith, S. J. (2016). Bench-scale and pilot-scale treatment technologies for the removal of total dissolved solids from coal mine water: A review. *Mine Water Environment*, *35*, 94–112. https://doi.org/10.1007/s10230-015-0351-7

Ramírez, M. E., Vélez, Y. H., Rendón, L., & Alzate, E. (2018). Potential of microalgae in the bioremediation of water with chloride content. *Brazilian Journal of Biology*, *78*(3), 472–476.

Rao, A. R., Dayananda, C., Sarada, R., Shamala, T. R., & Ravishankar, G. A. (2007). Effect of salinity on growth of green alga *Botryococcus braunii* and its constituents. *Bioresource Technology*, *98*, 560–564. https://doi.org/10.1016/j.biortech.2006.02.007

Renuka, N., Sood, A., Ratha, S. K., Prasanna, R., & Ahluwalia, A. S. (2013). Nutrient sequestration, biomass production by microalgae and phytoremediation of sewage water. *International Journal of Phytoremediation*, *15*, 789–800. https://doi.org/10.1080/15226514.2012.736436

Renuka, N., Sood, A., Ratha, S. K., Prasanna, R., & Ahluwalia, A. S. (2013). Evaluation of microalgal consortia for treatment of primary treated sewage effluent and biomass production. *Journal of Applied Phycology*, *25*, 1529–1537. https://doi.org/10.1007/s10811-013-9982-x

Schachtman, D. P., & Schroeder, J. I. (1994). Structure and transport mechanism of a high-affinity potassium uptake transporter from higher plants. *Nature*, *370*, 655–658. https://doi.org/10.1038/370655a0

Sheng, G. P., Yu, H. Q., & Li, X. Y. (2010). Extracellular polymeric substances (EPS) of microbial aggregates in biological wastewater treatment systems: A review. *Biotechnology Advances*, *28*, 882–894. https://doi.org/10.1016/j.biotechadv.2010.08.001

Silva, R., Cadorin, L., & Rubio, J. (2010). Sulphate ions removal from an aqueous solution: I. Co-precipitation with hydrolysed aluminum-bearing salts. *Minerals Engineering*, *23*(15), 1220–1226.

Song, Y., Hahn, H. H., & Hoffmann, E. (2002). Effect of solution conditions on the precipitation of phosphate for recovery: A thermaldynamic evaluation. *Chemosphere*, *48*, 1029–1034.

Steele, M. K., & Aitkenhead-Peterson, J. A. (2011). Long-term sodium and chloride surface water exports from the Dallas/Fort Worth region. *Science of the Total Environment*, *409*, 3021–3032. https://doi.org/10.1016/j.scitotenv.2011.04.015

Sydney, E. B., da Silva, T. E., Tokarski, A., Novak, A. C., de Carvalho, J. C., Woiciecohwski, A. L., … Soccol, C. R. (2011). Screening of microalgae with potential for biodiesel production and nutrient removal from treated domestic sewage. *Applied Energy*, *88*, 3291–3294. https://doi.org/10.1016/j.apenergy.2010.11.024

USEPA (2011). *Introduction to the National Pretreatment Program, EPA 430-R-115*.

Wang, M., Kuo-Dahab, W. C., Dolan, S., & Park, C. (2014). Kinetics of nutrient removal and expression of extracellular polymeric substances of the microalgae, *Chlorella* sp. and *Micractinium* sp., in wastewater treatment. *Bioresource Technology*, *154*, 131–137. https://doi.org/10.1016/j.biortech.2013.12.047

Weber-Scannell, P. K., & Duffy, L. K. (2007). Effects of total dissolved solids on aquatic organisms: A review of literature and recommendation for salmonid species. *American Journal of Environmental Sciences*, *3*(1), 1–6.

Xiao, R., & Zheng, Y. (2016). Overview of microalgal extracellular polymeric substances (EPS) and their applications. *Biotechnology Advances*, *34*, 1225–1244. https://doi.org/10.1016/j.biotechadv.2016.08.004

Zhang, C., Zhang, W., Huang, Y., & Gao, X. (2017). Analyzing the correlations of long-term seasonal water quality parameters, suspended solids and total dissolved solids in a shallow reservoir with meteorological factors. *Environmental Science and Pollution Research*, *24*, 6746–6756.

Zhao, X., Kumar, K., Gross, M., Kunetz, T., & Wen, Z. (2018). Evaluation of revolving algae biofilm reactors for nutrients and metals removal from sludge thickening supernatant in a municipal wastewater treatment facility. *Water Research*, *143*, 467–478. https://doi.org/10.1016/j.watres.2018.07.001

Zhou, H., Sheng, Y., Zhao, X., Gross, M., & Wen, Z. (2018). Treatment of acidic sulfate-containing wastewater using revolving algae biofilm reactors: Sulfur removal performance and microbial community characterization. *Bioresource Technology*, *264*, 24–34. https://doi.org/10.1016/j.biortech.2018.05.051

Zhou, W., Li, Y., Min, M., Hu, B., Zhang, H., Ma, X., … Ruan, R. (2012). Growing wastewater-borne microalga *Auxenochlorella protothecoides* UMN280 on concentrated municipal wastewater for simultaneous nutrient removal and energy feedstock production. *Applied Energy*, *98*, 433–440.

Zhou, W., Min, M., Li, Y., Hu, B., Ma, X., Cheng, Y., … Ruan, R. (2012). A hetero-photoautotrophic two-stage cultivation process to improve wastewater nutrient removal and enhance algal lipid accumulation. *Bioresource Technology*, *110*, 448–455. https://doi.org/10.1016/j.biortech.2012.01.063